

# Contrastive Learning for Image Complexity Representation

Shipeng Liu<sup>1</sup>, Liang Zhao<sup>1\*</sup>, Dengfeng Chen<sup>1</sup>, Zhanping Song<sup>1</sup>

<sup>1</sup>Xi'an University of Architecture and Technology

lsp@xauat.edu.cn, zhaoliang@xauat.edu.cn, chdengf@163.com, songzhpyt@xauat.edu.cn

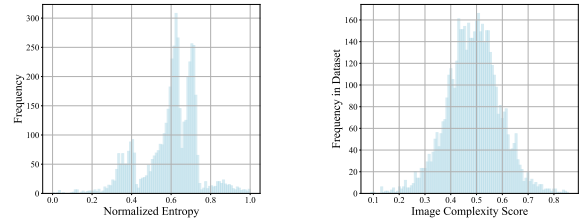
## Abstract

Quantifying and evaluating image complexity can be instrumental in enhancing the performance of various computer vision tasks. Supervised learning can effectively learn image complexity features from well-annotated datasets. However, creating such datasets requires expensive manual annotation costs. The models may learn human subjective biases from it. In this work, we introduce the MoCo v2 framework. We utilize contrastive learning to represent image complexity, named CLIC (Contrastive Learning for Image Complexity). We find that there are complexity differences between different local regions of an image, and propose Random Crop and Mix (RCM), which can produce positive samples consisting of multi-scale local crops. RCM can also expand the train set and increase data diversity without introducing additional data. We conduct extensive experiments with CLIC, comparing it with both unsupervised and supervised methods. The results demonstrate that the performance of CLIC is comparable to that of state-of-the-art supervised methods. In addition, we establish the pipelines that can apply CLIC to computer vision tasks to effectively improve their performance.

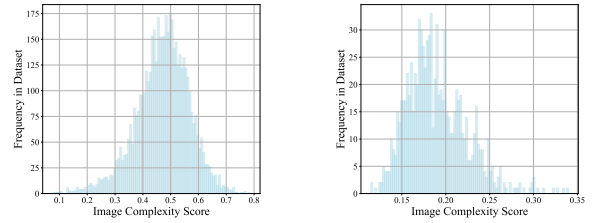
## Introduction

Image Complexity (IC) refers to describing the complexity level of an image. It is a relatively abstract concept that can be understood by humans (Forsythe 2009). Subjectively, image complexity is reflected in the diversity of visual elements, structural complexity, and the density of information, all of which collectively determine the difficulty for humans to cognize and understand an image (Heaps and Handel 1999). Objectively, IC can be considered as the various features within an image, such as color variations, texture distribution, and detail representation (Snodgrass and Vanderwart 1980). Consequently, IC is one of the important attributes that computer vision (CV) tasks, driven by image data, need to consider when processing images. In recent years, researchers have introduced the concept of computable image complexity. It refers to the simulation and quantification of human visual perception of image complexity by computer algorithms. The quantization and automatic prediction of image complexity has an important role and application in several fields. Such as understanding (Sarvamangala and

\*Corresponding Author.



(a) Global Entropy of MS COCO 2017 (Lin et al. 2014). (b) ICD of MS COCO 2017 (Lin et al. 2014).



(c) ICD of PASCAL VOC 2012 (Everingham et al. 2010). (d) ICD of Cornell Grasp (Jiang, Moseson, and Saxena 2011).

Figure 1: Image Complexity Distribution of Datasets.

Kulkarni 2022), object detection (Gong et al. 2021), UI design (Tuch et al. 2009), text detection (Grover et al. 2018), image enhancement (Li and Bai 2012). Therefore, accurate evaluation of IC is necessary to simulate human perception and facilitate subsequent tasks.

To accurately quantify and evaluate image complexity, some previous works focused on heuristic-based metrics such as information entropy (Yanyan, Huijuan, and Xinjiang 2016), image compression ratio (Li et al. 2021), and machine learning methods like SVM, random forests, and BP neural networks (Dai et al. 2022; Guo et al. 2018). However, these methods were primarily based on small-scale datasets and concentrated on handcrafted features, which limited their generalization ability in practical IC evaluation (Feng et al. 2022). With the advancement of deep learning and improved computational resources, deep convolutional neural networks (CNNs) have demonstrated strong capabilities in representation and generalization. CNNs can explicitly simulate human subjective perception in a data-driven

manner, such as image quality assessment (Su et al. 2020). Large-scale datasets and supervised learning-based methods for IC evaluation have also emerged, such as ComplexityNet (Kyle-Davidson, Bors, and Evans 2022a), ICNet (Feng et al. 2022), and ICCORN (Guo et al. 2023). Nevertheless, large-scale and well-annotated datasets require substantial human effort due to manual annotation of IC ground truth for each image. For instance, the authors of the IC9600 (Feng et al. 2022) organized a team of 7 people to score 9,600 images. The cost of such an approach is substantial. Although using the mean score as ground truth can mitigate subjective biases, supervised methods still inevitably introduce subjectivity.

If we aim to avoid costly annotation expenses and subjective biases, an intuitive idea is to utilize an unlabeled dataset for IC representation learning. Then we can use a few samples for fine-tuning to compute the IC score for each image. Self-supervised learning (SSL) (Liu et al. 2021a) generates pseudo-labels from unlabeled data, extracting useful information from the internal structure of the data, making it suitable for situations where labeled data is scarce. SSL can learn useful features from unlabeled data, reducing reliance on annotated datasets. The MoCo (He et al. 2020) framework marks a milestone in self-supervised learning for computer vision. MoCo employs a momentum encoder and a dynamic dictionary, utilizing contrastive learning to maximize the similarity between positive samples and minimize the similarity between positive and negative samples, addressing the issue of insufficient negative samples. The success of MoCo has sparked extensive follow-up research, such as MoCo v2 (Chen et al. 2020b), SimCLR (Chen et al. 2020a), BYOL (Grill et al. 2020), and SwAV (Caron et al. 2020). These methods have spurred the development of self-supervised contrastive learning, demonstrating tremendous potential in the field of computer vision.

To effectively evaluate image complexity while avoiding the expensive annotation costs and subjective biases, we propose CLIC based on the contrastive learning framework. CLIC learns image complexity features without annotations. We establish our image complexity representation learning framework based on the MoCo v2, utilizing contrastive learning to model the IC features of each image. Addressing the problem of local differences in image complexity, we introduce Random Crop and Mix (RCM). RCM generates positive samples by performing multi-scale random crop and mix the original images in the train set. We have validated the effectiveness of CLIC through extensive experiments, including comparisons with both unsupervised and supervised methods. Furthermore, we apply CLIC to fundamental computer vision tasks, and the results indicate that the performance of object detection and semantic segmentation tasks have been enhanced by aggregating the multi-scale image complexity features extracted from CLIC. In summary, we make the following contributions:

- We are the first to apply contrastive learning to model image complexity, eliminating the need for expensive annotations and completely avoiding human subjective biases.
- We propose the Random Crop and Mix, which generates

positive samples with both local and global features for contrastive learning.

- Our experiments show that CLIC achieves results close to those of supervised methods, and its performance significantly surpasses supervised methods when only a few samples are available. Additionally, CLIC, as an auxiliary prior, can enhance the performance of fundamental computer vision tasks.

## Related Works

### Image Complexity Evaluation

**Traditional Manual Method.** Chipman *et al.* (Chipman 1977) conducted early research on the factors contributing to the complexity of visual patterns, finding that structural features like similarity transformations and color transformations can reduce perceived complexity. Ichikawa *et al.* (Ichikawa 1985) and Oliva *et al.* (Olivia et al. 2004) studied the intrinsic processes underlying human judgments of pattern complexity, exploring how visual complexity in the real world is recognized by the human perceptual system. Rosenholtz *et al.* (Rosenholtz, Li, and Nakano 2007) proposed three methods to measure visual clutter, which is also a manifestation of image complexity. Ramanarayanan *et al.* (Ramanarayanan et al. 2008) used multidimensional scaling (MDS) to analyze subjects’ judgments of scene complexity. Chikhman *et al.* (Chikhman et al. 2012) established computational models using feature analysis methods such as spatial and frequency features to estimate image complexity, comparing these results with observers’ assessments. Palumbo *et al.* (Palumbo et al. 2014) and Machado *et al.* (Machado et al. 2015) both quantified visual complexity based on image compression algorithms, using correlation analysis to assess the difference between the quantified results and subjective complexity.

**Intelligent Learning Method.** Nagle *et al.* (Nagle and Lavie 2020) utilized a pre-trained convolutional neural network (CNN) to predict complexity scores for 4,000 images, achieving results highly correlated with human observer ratings. Saraee *et al.* (Saraee, Jalal, and Betke 2020) explored extracting unsupervised information from the intermediate convolutional layers of CNNs and proposed an activation energy metric to quantify visual complexity. Kyle-Davidson *et al.* (Kyle-Davidson, Bors, and Evans 2022b) used region adjacency graph cut algorithms to capture visually salient areas in images, calculated local symmetry to extract symmetry features, and established ComplexityNet to predict image complexity. Feng *et al.* (Feng et al. 2022) constructed a well-labeled image complexity evaluation dataset of 9,600 images at a high annotation cost and provided a baseline model, ICNet, for predicting image complexity scores and estimating complexity heatmaps in a weakly supervised manner. Guo *et al.* (Guo et al. 2023) argued that ICNet neglected the ordinal property of complexity scores and combined Deep Ordinal Regression with a larger network to assess image complexity. Shen *et al.* (Shen et al. 2023) used the SAM (Kirillov et al. 2023) and FC-CLIP (Yu et al. 2024) models to extract segments and category counts from images, constructing a linear model to fit image complexity.

## Contrastive Learning

InstDisc (Wu et al. 2018) is one of the early methods in contrastive learning, which achieved preliminary representation learning by treating each image instance as a unique category in an unsupervised manner. MoCo (He et al. 2020) used a momentum encoder to build a dynamic negative sample pool, addressing the issue of insufficient negative samples in small-batch training. MoCo stored and updated negative samples through momentum updates in a queue, allowing contrastive learning to perform well in small-batch settings. SimCLR (Chen et al. 2020a) generated positive sample pairs from different views of the same image through data augmentation, enhancing learning effectiveness with large-scale batch processing and a projection head network. Its innovation lies in the data augmentation strategy and large-scale training. MoCo v2 (Chen et al. 2020b) improved upon MoCo, adding a projection head similar to SimCLR to enhance learning effectiveness, and introducing stronger data augmentation, a larger model, and more training tricks to further boost performance. SwAV (Caron et al. 2020) conducted contrastive learning through clustering, using the clustering results of images from different views as the contrastive target. BYOL (Grill et al. 2020) achieved representation self-guided learning through the alternating training of two networks (online network and target network), demonstrating high-quality representation learning without explicit negative sample pairs. DINO (Zhang et al. 2022) used a self-supervised distillation method to transfer knowledge from a teacher network to a student network, achieving efficient learning without labels.

## Preliminary

### Definition of Image Complexity

Image complexity is a challenge to define. Traditional manual methods can calculate it using metrics such as image entropy and image compression ratio, but most are based on heuristic indicators, leading to inaccurate evaluations and limited generalization ability. Machine learning methods, on the other hand, model image complexity through supervised learning with high annotation costs, inevitably learning human subjective biases in the process. However, whether using manual or machine learning methods, image complexity modeling can be defined as in Eq.1, where  $x_i$  represents an image from a certain dataset, and  $f(\cdot)$  denotes the mapping function from this image to its image complexity  $IC_i$ , with the range of  $IC_i$  being 0 to 1.

$$IC_i = f(x_i) \quad (1)$$

After analyzing the image complexity of several datasets, we observed that, in general, the Image Complexity Distribution (ICD) of a dataset tends to approximate a normal distribution:

$$IC_i \sim N(\mu, \sigma^2) \quad (2)$$

Normal distribution indicates that the complexity score of most images cluster at a medium level. As shown in Figure 1, the ICDs calculated based on image entropy (Figure 1.(a)) and machine learning methods (Figure 1.(b,c,d)) both

IC Range	AP	$AP_{50}$	$AP_{75}$
All	40.5	59.3	43.8
<0.3	41.2 <sub>(+0.7)</sub>	60.3 <sub>(+1.0)</sub>	44.6 <sub>(+0.8)</sub>
>0.7	39.6 <sub>(-0.9)</sub>	58.0 <sub>(-1.3)</sub>	42.6 <sub>(-1.2)</sub>

Table 1: Results of YOLOX-S on MS COCO with different IC range. The training details for YOLOX-S were maintained consistent with the official implementation. All represents the original MS COCO val set, with the IC ranger from 0 to 1.

exhibit distribution curves that essentially fall within the category of normal distribution. It is worth noting that datasets (Figure 1.(b,c)) with such normally distributed ICDs are predominantly composed of natural scene images, such as streets, indoor, outdoor, and fields. However, some datasets, like the Cornell Grasp Dataset (Jiang, Moseson, and Saxena 2011), have a high frequency of ICD values concentrated around 0.17 (Figure 1.(d)), which is one of the reasons for the lower learning difficulty of these tasks (when only using the Cornell Grasp Dataset for 2D object detection tasks).

### Impaction of Image Complexity

We let ICNet (Feng et al. 2022) inference to sample images with IC below 0.3 and above 0.7 as our validation set on the MS COCO (Lin et al. 2014). Each complexity range contains 5,000 images, forming two training-validation set pairs. We trained on each training-validation set pair using a pre-trained YOLOX-S (Ge et al. 2021), and the results are presented in Table 1. The results clearly show that when IC is less than 0.3, the AP increases, and when IC is greater than 0.7, the AP decreases, indicating that the lower the image complexity, the easier the task, and the better the performance achieved. Therefore, modeling image complexity and applying it appropriately to fundamental computer vision tasks (such as detection and segmentation) is quite important. Feng *et al.* (Feng et al. 2022) have also demonstrated this phenomenon through extensive experiments.

## Method

### Contrastive Learning for Image Complexity

The IC9600 dataset incurred a high cost for manual annotation to generate IC scores for each image, and using supervised learning to train on it inevitably introduces subjective biases. Therefore, the motivation for this work is straightforward: to apply unsupervised learning to the representation learning of image complexity, thereby avoiding the high annotation costs and subjective biases.

MoCo v2 (Chen et al. 2020b) is an effective contrastive learning method that can learn useful representations from images without the high-cost annotation, it is also an unsupervised methods. MoCo v2, through contrastive learning between positive and negative samples, enables the model to train on a large amount of unlabeled data, extracting deep features from the images. We introduce the MoCo v2 framework and apply it to the unlabeled IC9600 dataset for representation learning of image complexity. Our method is

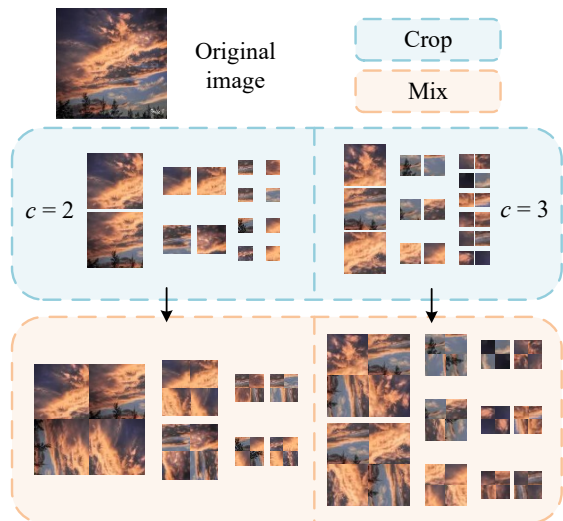


Figure 2: Image Random Crop and Mix (RCM). When  $c$  is 2 and 3, we get 14 and 21 crops, respectively. Then we mix 2 original crops in same size and their 2 transformed crops. We finally get 7 and 11 new images, respectively.

named CLIC. We experiment with two approaches to classify the training samples. The first one is to produce several groups of images through feature dimensionality reduction and clustering, where images within the same group were considered to have similar IC scores. However, our experiments demonstrate that there are significant differences within these groups. The second approach is to treat each image as a separate group for training. Since almost no two images have the same IC score, treating each image as an individual group is more intuitive. This also aligns with the classification approach in MoCo and MoCo v2, such as treating the number of ImageNet categories as 1.28 million, rather than 1,000.

### Image Random Crop and Mix

When humans subjectively assess the complexity of an image, they often analyze the complexity of its various components. For instance, in an image featuring both sky and ground, humans generally perceive the ground to be more complex than the sky, leading to an averaged evaluation rating. However, if the sky is filled with clouds, the final complexity evaluation rating would be appropriately increased. Our study of images with different complexities in the IC9600 dataset yielded the following observation.

**Observation 1.** *The pixel distribution of most images is uneven, characterized by features such as pixel gray levels, the number of edge pixels, and color diversity. These features vary significantly across different local regions within a single image.*

During the model learning, the complexity modeling of these local regions is insufficient, and the representation of the image complexity is predominantly conducted at the global level for one image. Human analysis of image complexity takes into account both local and global aspects of an

image. Feng *et al.* (Feng et al. 2022) also addressed this issue by using a framework with two branches, each capturing detailed information and context information, respectively. They utilized large-scale and small-scale feature maps to obtain local and global representations, respectively. In light of this analysis, we propose the Image Random Crop and Mix (RCM) for multiple views data augmentation. Similar to SwAV (Caron et al. 2020), our method generates multiple views from a single original image as positive samples for contrastive learning. However, our approach differs in that after random crop, these views are transformed and then mixed. These transformations involve common data augmentation methods. RCM results in at least 7 positive samples, each containing multiple crops. During the MoCo learning process, the query encoder learns local complexity features. Since the cropped views are mixed, these samples retains a sense of global context.

As illustrated in Figure 2, we perform random region crop on an image, where the cropped regions are of different scales. In this paper, the scales used are  $L/c$ ,  $L/2c$  and  $L/4c$ , respectively. The number of cropped regions per image corresponding to each scale is  $c$ ,  $2c$ , and  $4c$ , respectively.  $L$  and  $c$  are defined as:

$$L = \min(H, W) \quad (3)$$

$$c \geq 2 \quad (4)$$

Where  $c$  is a hyperparameter. After cropping, the images undergo color transformation, rotation, and other common data augmentation processes before being combined to form several positive samples. During MoCo training, the several positive samples we produce are compared one by one with other negative samples, ultimately resulting in a combined loss value.

**RCM as A Data Expander.** In this work, we discover that RCM can not only be used to generate positive samples for contrastive learning but also acts as a data expander to increase the scale of the train set. This idea is intuitive, as we observe that the IC9600 dataset used for contrastive learning training is insufficient, given that training on large-scale benchmarks, like MoCo (He et al. 2020) and SimCLR (Chen et al. 2020a), often involves datasets with over a billion. Considering the severe limitation in the number of images in IC9600 dataset, we need to find a way to maximize the increase in the number of train images. Based on this perspective, we consider using RCM to expand the original IC9600 train set, which not only avoids the introduction of additional training data but also eliminates the need for human labor to re-screen suitable images. Note that when RCM is used for data expansion, positive samples are generated in the training phase in the same manner as before.

### Applying for CV Tasks

Related work and previous discussions have demonstrated that images with higher complexity scores are more challenging in fundamental computer vision tasks, such as detection and segmentation. Utilizing image complexity scores or complexity maps to assist computer vision tasks can enhance their performance. For instance, Feng *et al.* (Feng et al. 2022) applied visual complexity through multi-task

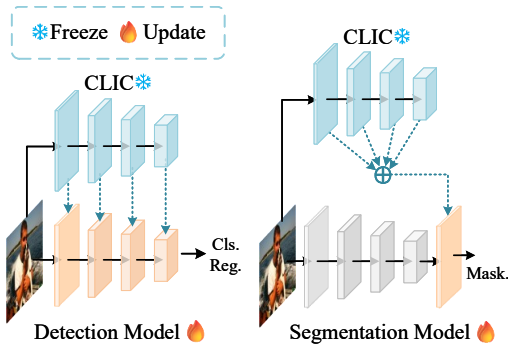


Figure 3: Pipelines of applying CLIC to CV tasks (object detection and semantic segmentation). Cls and Reg indicate heads of object detection. Mask is the head of semantic segmentation.

learning, multi-modal learning, and prior weighting. Multi-task learning requires calculating losses with the IC score ground truth to assist the main branch learning. The other two approaches essentially fuse the learned image complexity features into the main branch through feature fusion. Similarly, we further extend the application of image complexity feature fusion, utilizing multi-scale fusion to fully utilize the image complexity features.

We incorporate the query encoder trained by CLIC into the training process of detection or segmentation tasks by freezing its parameters. During training, CLIC does not participate in the backpropagation process, as shown in Figure 3. In the fusion phase of object detection, we align the scales of CLIC to the backbone or neck of the detection framework, adding skip connections at each stage. This method integrates the image complexity features extracted by the CLIC as auxiliary prior information into the learning of the detection model. For semantic segmentation, we use the ASPP (Atrous Spatial Pyramid Pooling) from DeepLab v3 (Chen et al. 2018) to fuse the features of CLIC at different scales, then concatenate them to the segmentation head.

## Experiment

### Setup

We utilized 4 NVIDIA GTX 3090 GPUs to conduct all experiments. CLIC was trained using the MoCo v2 framework, and the fine-tuning of CLIC was based on the ICNet (Feng et al. 2022) framework.

**Train Detail.** We train CLIC on MoCo v2. All backbones are pretrained with ImageNet. The batch size is 128, the initial learning rate is 0.03. All models have trained 200 epochs, where the learning rate is reduced by a factor of 10 at the 120th and the 160th epoch. The MoCo momentum for updating the key encoder is 0.999. The softmax temperature is 0.2. Other settings are kept consistent with MoCo v2.

**Fine-tuning Details.** We fine-tuning CLIC on ICNet. The parameters of CLIC are frozen during fine-tuning. The batch size is 128. Stochastic Gradient Descent (SGD) is used to optimize the model. The momentum is 0.9, and the weight

Method		PCC $\uparrow$	SRCC $\uparrow$
Unsup.	SE	0.534	0.498
	NR	0.556	0.541
	ED	0.569	0.491
	AR	0.571	0.481
	UAE	<b>0.651</b>	<b>0.635</b>
Super.	SAE	0.865	0.860
	ComplexityNet $\dagger$	0.873	0.870
	HyperIQA	0.935	0.935
	P2P-FM	0.940	0.936
	ICNet $\dagger$	0.947	0.944
	ICCORN	<b>0.954</b>	<b>0.951</b>
CLIC	Res18	0.882	0.878
	Res152	0.891	0.889
	Swin-B	0.905	0.902
	Swin-B+RCM	0.912	0.909
	Swin-B+RCM $\ddagger$	<b>0.919</b>	<b>0.916</b>

Table 2: Comparison with other method.  $\dagger$  indicates our replication results, and results without this symbol were obtained from Feng *et al.* (Feng et al. 2022).  $\ddagger$  indicates that RCM was used for dataset augmentation, with  $c$  set to 2 for RCM. Unsup represents unsupervised learning methods, and Super represents supervised learning methods.

decay is 0.001. The learning rate is fixed at 0.001. All models have trained 30 epochs. Other settings are kept consistent with ICNet.

### CLIC vs. Unsupervised & Supervised

We compare CLIC with other methods for evaluating image complexity, including both unsupervised and supervised methods. We use the same metrics as Feng *et al.* (Feng et al. 2022), namely the Pearson correlation coefficient (PCC) (Guo et al. 2013) and Spearman’s rank correlation coefficient (SRCC) (Chen et al. 2015). Our CLIC is trained by the MoCo v2 framework. Then we set the query encoder as the backbone for ICNet. We fine-tuning the two heads on IC9600 dataset by freezing CLIC parameters, the results are presented in Table 2. Note that ICNet employs a dual-branch structure, whereas our CLIC is a standalone branch.

From the metrics results in Table 2, UAE in the unsupervised group show the best result, but there is a significant gap to ICCORN (Guo et al. 2023) in the supervised group. Note, the unsupervised methods are mostly based on traditional heuristic indicators designed manually. In contrast, most supervised methods are deep learning-based and achieve much better performance than the unsupervised methods. This is due to the great advantages of deep learning for feature extraction. Although our CLIC do not achieve a similar performance to the supervised methods, we aim to address the expensive labeling cost and avoid subjective bias. Furthermore, when we replace the query-key encoder with larger scale networks, the PCC and SRCC continued to increase. In particular, the PCC and SRCC using the combination of Swin-B (Liu et al. 2021b) and RCM $\ddagger$  reach 0.919 and 0.916, respectively. This is very close to supervised methods.

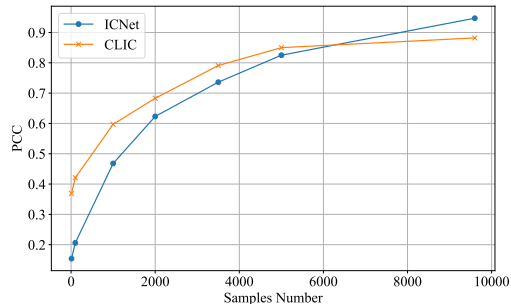


Figure 4: Performance with different samples number.

### Contributions of Samples Number

We apply MoCo v2 to image complexity representation and then fine-tuning with a little number of samples. Here, we compare CLIC with the supervised method ICNet by gradually increasing the number of samples for fine-tuning, as shown in Figure 4. Note that ICNet is trained from scratch with the same number of samples instead of fine-tuning.

Firstly, both methods show expected improvements in performance as the number of samples increases. Then, we observe that CLIC, from the start with only 10 samples, achieves nearly 0.4 PCC, while ICNet only reaches around 0.1. As the sample number increased, CLIC is gradually close to saturation at 5k samples. This is due to fine-tuning only updating the head while the feature extraction parameters are fixed. However, this trend demonstrates that CLIC can quickly enhance its image complexity representation results with only a small number of samples for fine-tuning. This proves the effectiveness of our method. Finally, we find that when enough samples are used, the accuracy of ICNet far exceeds that of CLIC. This also indicates the crucial importance of a well-annotated train set for model learning.

### Ablation: RCM

The RCM can be used not only to generate positive samples but also to expand the train set. We observed an interesting phenomenon. In Table 2, the result of RCM used for dataset expansion (Swin-B+RCM $\ddagger$ ) is better than RCM used to generate positive samples (Swin-B+RCM), with 0.919 and 0.912 PCC, respectively. This result suggests that RCM might be more suitable for dataset expansion. We speculate that there are two reasons for this outcome. Firstly, SwAV, after generating multiple view positive samples, matches them with its unique cluster centers, which can constrain the optimization direction of contrastive learning. Secondly, our train set might be too small. As contrastive learning methods like MoCo and SwAV are typically trained on large-scale benchmarks, the IC9600 dataset lacks sufficient image diversity.

We further conduct an ablation study on the two usages of RCM with different values of  $c$ . The ablation results for RCM used to generate positive samples are shown in Table 3. When  $c$  is 0, meaning RCM is not used, there is only one positive sample. When  $c$  is 2 or 3, 7 and 11 positive

$c$ of RCM	Positives	PCC $\uparrow$	SRCC $\uparrow$
0	1	0.882	0.878
2	7	<b>0.889</b>	<b>0.886</b>
3	11	0.885	0.880

Table 3: Results of RCM for generate positive samples.

$c$ of RCM $\ddagger$	Scale of Train Set	PCC $\uparrow$	SRCC $\uparrow$
0	1 $\times$	0.882	0.878
2	7 $\times$	0.895	0.892
3	11 $\times$	<b>0.897</b>	<b>0.894</b>
4	14 $\times$	0.875	0.871
5	18 $\times$	0.841	0.837

Table 4: Results of RCM for expanding train set.

samples are produced, respectively. The corresponding PCC and SRCC are also improved. However, the metrics are best when  $c$  is 2. The metrics start to decrease when  $c$  is 3. We analyze the reason for this is that an increase in  $c$  leads to progressively smaller crops. The combination of features with too small crops will be more cluttered, which will lead to optimization in the wrong direction of contrastive learning.

The ablation results of RCM used for dataset expansion are presented in Table 4. We find that as  $c$  gradually increases, the scale of the training set rapidly increases from the original 1 $\times$  to 18 $\times$ . The corresponding number of images used for training jumps from about 10k to about 180k. Furthermore, we observe that when  $c$  is 3, PCC and SRCC reach their highest scores, at 0.897 and 0.894, respectively. However, when  $c$  continues to increase, the metrics begin to decline rapidly. The reason for this phenomenon is that the original number of images is only about 10k. When the number of images reaches about 140k or more, the train set is almost dominated by generated images (which can be considered as pseudo images). An excessive number of pseudo images can severely interfere with the positive value brought by real data.

To validate the performance limitations due to the small scale of the train set, we utilize similarity calculation to obtain extra data from datasets or websites such as MS COCO, PASCAL VOC, and Google. Note that all these extra images are matched for similarity with a few of the images from each group in IC9600. Thus none of the extra images we acquired were manually filtered and possessed more or less similar features to those of the IC9600. The results are presented in Table 5. It is clear that as the amount of extra data continues to increase, both PCC and SRCC continue to improve.

### Results of Application Pipelines.

**Applying for Detection.** We apply our CLIC to Mask R-CNN[52] with several backbone. The train details are same as MMDetection[53]. The results are shown in Table 6. Overall, the addition of image complexity features improves the performance of the detection model. However, as the backbone of Mask R-CNN continues to deepen, the enhancement brought by CLIC continues to decay. We con-

Extra Data	PCC $\uparrow$	SRCC $\uparrow$
0	0.8824	0.8776
1k	0.8828	0.8779
3k	0.8833	0.8783
5k	0.8838	0.8788
10k	0.8846	0.8807
50k	<b>0.8921</b>	<b>0.8885</b>

Table 5: Results of introducing extra data for train with RCM( $c = 0$ ).

Backbone	AP	$AP_{50}$	$AP_{75}$
R-50	38.2	58.5	41.4
R-10	40.0	60.5	44.0
X-101-32x4d	41.9	62.5	45.9
R-50 $\dagger$	38.5 $_{(+0.3)}$	59.1 $_{(+0.6)}$	41.8 $_{(+0.4)}$
R-101 $\dagger$	40.2 $_{(+0.2)}$	60.9 $_{(+0.4)}$	44.2 $_{(+0.2)}$
X-101-32x4d $\dagger$	42.0 $_{(+0.1)}$	62.7 $_{(+0.2)}$	45.8 $_{(-0.1)}$
X-101-32x4d $\dagger\dagger$	42.3 $_{(+0.4)}$	63.3 $_{(+0.8)}$	46.5 $_{(+0.6)}$

Table 6: Comparison of Mask R-CNN on MS COCO. All models are trained with  $1\times$  learning rate schedule.  $\dagger$  indicate CLIC is applied. The CLIC weight of feature map which is add to FPN is 0.5. CLIC is a ResNet18 trained by MoCo v2 on IC9600 with RCM $\ddagger$ ( $c = 2$ ).  $\dagger\dagger$  means CLIC is a ResNet152.

sider that it may be because the ResNet18-based CLIC network has fewer layers and is less capable of extracting image features relative to ResNet50 and ResNet101. Therefore, we apply a CLIC based on ResNet152 to the X-101-32x4d in Table 6(X-101-32x4d $\dagger\dagger$ ). We expect to utilize a deeper network to obtain better image complexity features. The results confirmed our hypothesis, with the performance improvements of X-101-32x4d $\dagger\dagger$  being higher than those of X-101-32x4d $\dagger$ .

**Applying for Segmentation.** We apply our CLIC to FCN (Long, Shelhamer, and Darrell 2015) with R-50-D8. The train details are same as MMSegmentation (Contributors 2020). Compare to the FCN, the CLIC-assisted FCN $\dagger$  has a mIoU improvement of 1.98. This demonstrates the auxiliary optimization effect of image complexity on semantic segmentation tasks. However, we find that CLIC bring 9GB GPU memory consumption. Also the FPS is reduced by 4.38. This is a drawback of CLIC. Both the train and inference of FCN require CLIC, as the knowledge from CLIC cannot be transferred to FCN. Although concurrent execution (FCN $\dagger\dagger$ ) can improve running speed, it is negligible. Although the GPU memory consumption is almost the same for concurrent and sequential execution, the CPU and normal memory need to bear this additional burden. This is something to be avoided in practical engineering applications. We continue to visualize some results of the PASCAL VOC 2012 validation set in Figure 5, where the segmentation results of FCN $\dagger$  show a larger and more accurate coverage of the pixels for each object.

Method	Mem	FPS	mIoU
FCN	5.6G	19.64	66.53
FCN $\dagger$	14.5G	15.26 $_{(-4.38)}$	68.51 $_{(+1.98)}$
FCN $\dagger\dagger$	14.5G	17.83 $_{(-1.81)}$	68.50 $_{(+1.97)}$

Table 7: Comparison of FCN on PASCAL VOC 2012. The backbone of FCN is R-50-D8.  $\dagger$  indicate CLIC is applied. The CLIC weight of feature map which is add to FCN head is 0.5. CLIC is a ResNet101 trained by MoCo v2 on IC9600 with RCM $\ddagger$ ( $c = 2$ ). FCN $\dagger\dagger$  indicates the concurrent processing of CLIC and FCN.

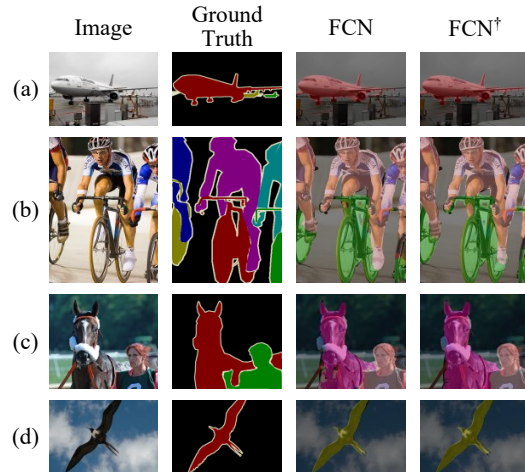


Figure 5: Visualization of FCN with PASCAL VOC 2012 val set.

## Conclusion

To accurately model image complexity, high-quality annotation, and supervised learning are typically preferred. However, this approach inevitably leads to issues such as high annotation costs and subjective biases. In this paper, we consider utilizing unsupervised learning to model image complexity, addressing these challenges. We introduce the MoCo v2 framework, which employs contrastive learning to train encoders in extracting image complexity features. Our experiments demonstrate the effectiveness of our proposed method, CLIC, which performs comparably to state-of-the-art supervised methods. Furthermore, the multi-scale application pipelines effectively enhance the performance of computer vision tasks.

## References

- Caron, M.; Misra, I.; Mairal, J.; Goyal, P.; Bojanowski, P.; and Joulin, A. 2020. Unsupervised learning of visual features by contrasting cluster assignments. *Advances in neural information processing systems*, 33: 9912–9924.
- Chen, L.-C.; Zhu, Y.; Papandreou, G.; Schroff, F.; and Adam, H. 2018. Encoder-decoder with atrous separable convolution for semantic image segmentation. In *Proceedings of the European conference on computer vision (ECCV)*, 801–818.

- Chen, T.; Kornblith, S.; Norouzi, M.; and Hinton, G. 2020a. A simple framework for contrastive learning of visual representations. In *International conference on machine learning*, 1597–1607. PMLR.
- Chen, X.; Fan, H.; Girshick, R.; and He, K. 2020b. Improved baselines with momentum contrastive learning. *arXiv preprint arXiv:2003.04297*.
- Chen, Y.-Q.; Duan, J.; Zhu, Y.; Qian, X.-F.; and Xiao, B. 2015. Research on the image complexity based on neural network. In *2015 International Conference on Machine Learning and Cybernetics (ICMLC)*, volume 1, 295–300. IEEE.
- Chikhman, V.; Bondarko, V.; Danilova, M.; Goluzina, A.; and Shelepin, Y. 2012. Complexity of images: Experimental and computational estimates compared. *Perception*, 41(6): 631–647.
- Chipman, S. F. 1977. Complexity and structure in visual patterns. *Journal of Experimental Psychology: General*, 106(3): 269.
- Contributors, M. 2020. MMSegmentation: Openmmlab semantic segmentation toolbox and benchmark.
- Dai, L.; Zhang, K.; Zheng, X. S.; Martin, R. R.; Li, Y.; and Yu, J. 2022. Visual complexity of shapes: a hierarchical perceptual learning model. *The Visual Computer*, 1–14.
- Everingham, M.; Van Gool, L.; Williams, C. K.; Winn, J.; and Zisserman, A. 2010. The pascal visual object classes (voc) challenge. *International journal of computer vision*, 88: 303–338.
- Feng, T.; Zhai, Y.; Yang, J.; Liang, J.; Fan, D.-P.; Zhang, J.; Shao, L.; and Tao, D. 2022. IC9600: a benchmark dataset for automatic image complexity assessment. *IEEE Transactions on Pattern Analysis and Machine Intelligence*, 45(7): 8577–8593.
- Forsythe, A. 2009. Visual complexity: Is that all there is? In *Engineering Psychology and Cognitive Ergonomics: 8th International Conference, EPCE 2009, Held as Part of HCI International 2009, San Diego, CA, USA, July 19-24, 2009. Proceedings 8*, 158–166. Springer.
- Ge, Z.; Liu, S.; Wang, F.; Li, Z.; and Sun, J. 2021. YoloX: Exceeding yolo series in 2021. *arXiv preprint arXiv:2107.08430*.
- Gong, Y.; Yu, X.; Ding, Y.; Peng, X.; Zhao, J.; and Han, Z. 2021. Effective fusion factor in FPN for tiny object detection. In *Proceedings of the IEEE/CVF winter conference on applications of computer vision*, 1160–1168.
- Grill, J.-B.; Strub, F.; Altché, F.; Tallec, C.; Richemond, P.; Buchatskaya, E.; Doersch, C.; Avila Pires, B.; Guo, Z.; Gheshlaghi Azar, M.; et al. 2020. Bootstrap your own latent: a new approach to self-supervised learning. *Advances in neural information processing systems*, 33: 21271–21284.
- Grover, R.; Yadav, D. K.; Chauhan, D.; and Kamya, S. 2018. Adaptive steganography via image complexity analysis using 3D color texture feature. In *2018 3rd International Innovative Applications of Computational Intelligence on Power, Energy and Controls with their Impact on Humanity (CIPECH)*, 1–5. IEEE.
- Guo, X.; Kurita, T.; Asano, C. M.; and Asano, A. 2013. Visual complexity assessment of painting images. In *2013 IEEE International Conference on Image Processing*, 388–392. IEEE.
- Guo, X.; Qian, Y.; Li, L.; and Asano, A. 2018. Assessment model for perceived visual complexity of painting images. *Knowledge-Based Systems*, 159: 110–119.
- Guo, X.; Wang, L.; Yan, T.; and Wei, Y. 2023. Image Visual Complexity Evaluation Based on Deep Ordinal Regression. In *Chinese Conference on Pattern Recognition and Computer Vision (PRCV)*, 199–210. Springer.
- He, K.; Fan, H.; Wu, Y.; Xie, S.; and Girshick, R. 2020. Momentum contrast for unsupervised visual representation learning. In *Proceedings of the IEEE/CVF conference on computer vision and pattern recognition*, 9729–9738.
- Heaps, C.; and Handel, S. 1999. Similarity and features of natural textures. *Journal of Experimental Psychology: Human Perception and Performance*, 25(2): 299.
- Ichikawa, S. 1985. Quantitative and structural factors in the judgment of pattern complexity. *Perception & psychophysics*, 38(2): 101–109.
- Jiang, Y.; Moseson, S.; and Saxena, A. 2011. Efficient grasping from rgb-d images: Learning using a new rectangle representation. In *2011 IEEE International conference on robotics and automation*, 3304–3311. IEEE.
- Kirillov, A.; Mintun, E.; Ravi, N.; Mao, H.; Rolland, C.; Gustafson, L.; Xiao, T.; Whitehead, S.; Berg, A. C.; Lo, W.-Y.; et al. 2023. Segment anything. In *Proceedings of the IEEE/CVF International Conference on Computer Vision*, 4015–4026.
- Kyle-Davidson, C.; Bors, A. G.; and Evans, K. K. 2022a. Predicting human perception of scene complexity. In *2022 IEEE International Conference on Image Processing (ICIP)*, 1281–1285. IEEE.
- Kyle-Davidson, C.; Bors, A. G.; and Evans, K. K. 2022b. Predicting human perception of scene complexity. In *2022 IEEE International Conference on Image Processing (ICIP)*, 1281–1285. IEEE.
- Li, M.; and Bai, M. 2012. A mixed edge based text detection method by applying image complexity analysis. In *Proceedings of the 10th World Congress on Intelligent Control and Automation*, 4809–4814. IEEE.
- Li, P.; Yang, Y.; Zhao, W.; and Zhang, M. 2021. Evaluation of image fire detection algorithms based on image complexity. *Fire safety journal*, 121: 103306.
- Lin, T.-Y.; Maire, M.; Belongie, S.; Hays, J.; Perona, P.; Ramanan, D.; Dollár, P.; and Zitnick, C. L. 2014. Microsoft coco: Common objects in context. In *Computer Vision—ECCV 2014: 13th European Conference, Zurich, Switzerland, September 6-12, 2014, Proceedings, Part V 13*, 740–755. Springer.
- Liu, X.; Zhang, F.; Hou, Z.; Mian, L.; Wang, Z.; Zhang, J.; and Tang, J. 2021a. Self-supervised learning: Generative or contrastive. *IEEE transactions on knowledge and data engineering*, 35(1): 857–876.

- Liu, Z.; Lin, Y.; Cao, Y.; Hu, H.; Wei, Y.; Zhang, Z.; Lin, S.; and Guo, B. 2021b. Swin transformer: Hierarchical vision transformer using shifted windows. In *Proceedings of the IEEE/CVF international conference on computer vision*, 10012–10022.
- Long, J.; Shelhamer, E.; and Darrell, T. 2015. Fully convolutional networks for semantic segmentation. In *Proceedings of the IEEE conference on computer vision and pattern recognition*, 3431–3440.
- Machado, P.; Romero, J.; Nadal, M.; Santos, A.; Correia, J.; and Carballal, A. 2015. Computerized measures of visual complexity. *Acta psychologica*, 160: 43–57.
- Nagle, F.; and Lavie, N. 2020. Predicting human complexity perception of real-world scenes. *Royal Society open science*, 7(5): 191487.
- Olivia, A.; Mack, M. L.; Shrestha, M.; and Peeper, A. 2004. Identifying the perceptual dimensions of visual complexity of scenes. In *Proceedings of the annual meeting of the cognitive science society*, volume 26.
- Palumbo, L.; Ogden, R.; Makin, A. D.; and Bertamini, M. 2014. Examining visual complexity and its influence on perceived duration. *Journal of vision*, 14(14): 3–3.
- Ramanarayanan, G.; Bala, K.; Ferwerda, J. A.; and Walter, B. 2008. Dimensionality of visual complexity in computer graphics scenes. In *Human vision and electronic imaging xiii*, volume 6806, 142–151. SPIE.
- Rosenholtz, R.; Li, Y.; and Nakano, L. 2007. Measuring visual clutter. *Journal of vision*, 7(2): 17–17.
- Saraee, E.; Jalal, M.; and Betke, M. 2020. Visual complexity analysis using deep intermediate-layer features. *Computer Vision and Image Understanding*, 195: 102949.
- Sarvamangala, D.; and Kulkarni, R. V. 2022. Convolutional neural networks in medical image understanding: a survey. *Evolutionary intelligence*, 15(1): 1–22.
- Shen, T.; Nath, S. S.; Brielmann, A.; and Dayan, P. 2023. Simplicity in Complexity: Explaining Visual Complexity using Deep Segmentation Models. In *Proceedings of the Annual Meeting of the Cognitive Science Society*, volume 46.
- Snodgrass, J. G.; and Vanderwart, M. 1980. A standardized set of 260 pictures: norms for name agreement, image agreement, familiarity, and visual complexity. *Journal of experimental psychology: Human learning and memory*, 6(2): 174.
- Su, S.; Yan, Q.; Zhu, Y.; Zhang, C.; Ge, X.; Sun, J.; and Zhang, Y. 2020. Blindly assess image quality in the wild guided by a self-adaptive hyper network. In *Proceedings of the IEEE/CVF conference on computer vision and pattern recognition*, 3667–3676.
- Tuch, A. N.; Bargas-Avila, J. A.; Opwis, K.; and Wilhelm, F. H. 2009. Visual complexity of websites: Effects on users' experience, physiology, performance, and memory. *International journal of human-computer studies*, 67(9): 703–715.
- Wu, Z.; Xiong, Y.; Yu, S. X.; and Lin, D. 2018. Unsupervised feature learning via non-parametric instance discrimination. In *Proceedings of the IEEE conference on computer vision and pattern recognition*, 3733–3742.
- Yanyan, C.; Huijuan, W.; and Xinjiang, M. 2016. Digital image enhancement method based on image complexity. *International Journal of Hybrid Information Technology*, 9(6): 395–402.
- Yu, Q.; He, J.; Deng, X.; Shen, X.; and Chen, L.-C. 2024. Convolutions die hard: Open-vocabulary segmentation with single frozen convolutional clip. *Advances in Neural Information Processing Systems*, 36.
- Zhang, H.; Li, F.; Liu, S.; Zhang, L.; Su, H.; Zhu, J.; Ni, L. M.; and Shum, H.-Y. 2022. Dino: Detr with improved denoising anchor boxes for end-to-end object detection. *arXiv preprint arXiv:2203.03605*.